Progress in Additive Manufacturing
https://doi.org/10.1007/s40964-024-00780-0

FULL RESEARCH ARTICLE

Unlocking the potential of low-melting-point alloys integrated extrusion additive manufacturing: insights into mechanical behavior, energy absorption, and electrical conductivity

Liuchao Jin[1,2,3] · **Xiaoya Zhai**[4] · **Kang Zhang**[1] · **Jingchao Jiang**[5]

Received: 17 May 2024 / Accepted: 28 August 2024

Abstract

Additive manufacturing is a commonly used manufacturing method in complex part fabrication, instant assemblies, part consolidation, mass customization and personalization, on-demand manufacturing, lightweight, and topological optimization due to its advantage of lower costs, flexibility to learn and use, reduced raw material wastage, digital design integration, high efficiency, environmental-friendliness. However, the current metal 3D printing, which is mainly fabricated layer by layer using laser, is expensive to manufacture metal parts. Therefore, in this paper, a low-cost high-quality metal manufacturing process called low-melting-point alloys (LMPAs) integrated extrusion additive manufacturing will be examined. This manufacturing process can fabricate complex metal structures and integrated circuits with simple fused deposition modeling, which is a cost-effective method for producing these objects. LMPAs with different melting points are used for performance comparison to find out the optimized mechanical behavior, energy absorption properties, and electrical conductivity. Our investigation into LMPAs integrated extrusion additive manufacturing has revealed significant findings. Tensile tests conducted on LMPAs with varying melting points have illuminated distinct mechanical behaviors. Notably, lower melting points contribute to increased ductility but reduced stiffness, while higher melting points result in greater stiffness but diminished ductility. These results emphasize the importance of tailoring LMPA selection based on specific application requirements. Furthermore, our examination of lattice and triply periodic minimal surface structures has demonstrated consistent energy absorption properties across different manufacturing temperatures, highlighting the adaptability and versatility of LMPAs for energy absorption applications. Additionally, our electrical conductivity assessments have shown that LMPAs with melting points of $47^{\circ}C$ and 120°C exhibit higher electrical conductivity, making them suitable for applications requiring good electrical conduction properties. These findings collectively underscore the significance of LMPAs in additive manufacturing, offering valuable insights for material selection and applications in various domains.

Keywords Additive manufacturing · 3D printing · Low-melting-point alloys · Smart manufacturing

✉ Jingchao Jiang
j.jiang2@exeter.ac.uk

Liuchao Jin
liuchao.jin@link.cuhk.edu.hk

Xiaoya Zhai
xiaoyazhai@ustc.edu.cn

Kang Zhang
1155173007@link.cuhk.edu.hk

[1] Department of Mechanical and Automation Engineering, The Chinese University of Hong Kong, Hong Kong, China

[2] Shenzhen Key Laboratory of Soft Mechanics & Smart Manufacturing, Southern University of Science and Technology, Shenzhen 518055, China

[3] Department of Mechanical and Energy Engineering, Southern University of Science and Technology, Shenzhen 518055, China

[4] School of Mathematical Sciences, University of Science and Technology of China, Hefei 230026, China

[5] Department of Engineering, University of Exeter, Exeter, UK

Published online: 09 September 2024

1 Introduction

Since the inception of 3D printing technology in the 1980 s, it has undergone rapid advancements and witnessed numerous innovations [1, 2]. This transformative technology has unlocked a vast array of printing materials, providing researchers with a diverse palette that includes polymers [3–11], metals [12–15], ceramics [16–20], concrete [21–23], ice [24–26], wood [27–29], and even sugar [30, 31]. Among these materials, metal printing has emerged as a standout due to its inherent advantages, including rapid prototyping capabilities, high production efficiency, minimized material wastage, manufacturing flexibility, and the ability to craft intricate and complex designs. However, it is important to note that most traditional metal printing processes are grounded in techniques such as powder bed fusion [32–36], direct energy deposition [37–42], and binder jetting [43, 44]. These techniques primarily involve layer-by-layer sintering of metal powder using a laser, electron beam, or energy injection. However, the cost associated with metal printing, encompassing both the machines and the raw materials [45], renders it economically prohibitive for many industries and manufacturers.

Contrastingly, the advent of low melting point alloys (LMPAs), also known as fusible alloys, has ushered in the prospect of resolving some of the inherent limitations of Direct Metal Laser Sintering (DMLS) and making metal printing more accessible and cost-effective. LMPAs are characterized by their unique chemical compositions, enabling them to melt at low temperatures and subsequently resolidify. Notably, these alloys empower the production and casting of components at temperatures below 300 degrees Celsius. Furthermore, LMPAs exhibit remarkable electrical and thermal conductivity, further broadening their applications across various domains, including flexible circuits [46–49], advanced electronics [50–57], thermal conduction [58–60], energy harvesting [61–63], smart structures [64, 65], and bio-medicine [66].

Numerous research endeavors have been devoted to the exploration of nozzle-based direct printing of LMPAs, whereby layers are intricately deposited along a predetermined path. These printing methodologies encompass fused deposition modeling (FDM) and electrohydrodynamic (EHD) inkjet printing. Li et al. [67] pioneered the development of an FDM 3D printer designed explicitly for LMPAs part production, focusing primarily on the structural design of the printer. However, their work was limited to the design phase, lacking the verification of actual LMPAs part fabrication feasibility. In contrast, Hsieh et al. [68] proposed an FDM approach tailored to LMPAs, enabling the direct extrusion of LMPAs onto a platform. Their pioneering work demonstrated the feasibility of this approach by successfully printing lines and layers. However, the challenge of printing complex structures remained unaddressed, and the quality of the resulting LMPAs parts was suboptimal, featuring a rough surface finish and difficulty in controlling the extrusion amount of LMPAs. Parvanda and Kala [69] also explored FDM for LMPAs printing, undertaking an investigation into the process window by identifying parameters such as print speeds, temperatures, filament lengths, and layer heights conducive to LMPAs printing. However, the quality of prints, particularly in terms of layer heights, remained unsatisfactory, and complex part fabrication was unattained. Ladd et al. [70] introduced a 3D LMPAs micro-structure direct-write method, offering the capability to print wires, spherical arrays, arches, and interconnects. Despite this innovation, precision in printing was not yet optimal, and limitations persisted regarding the complexity of printed structures. Yu et al. [71] ventured into direct printing of LMPAs in a variety of macroscopic 3D structures at room temperature via an adhesive process. Their work involved characterizing the layer stacking process and assessing the stability of layer thickness ranges and printing speed. Nonetheless, layer stacking introduced unsatisfactory adhesion between layers, adversely affecting the mechanical properties of printed parts in the vertical direction. Yu et al. [72] explored a novel conceptual technique known as suspension 3D printing for LMPAs, employing self-healing hydrogel support to create macroscopic LMPAs structures. While this method demonstrated promise, it suffered from challenges related to controlling the extrusion amount of LMPAs inside the nozzle and featured minimal adhesion between successive layers. Deng et al. [64] presented a hybrid manufacturing process combining 3D printing, vacuum casting, and conformal coating techniques to fabricate multifunctional LMPAs lattice materials. This approach yielded high-quality lattice structures with shape memory effects. However, the complexity and resource-intensive nature of the manufacturing process, involving seven distinct steps and elevated temperatures for certain processes, posed significant drawbacks. Huang et al. [73] harnessed EHD inkjet printing to produce LMPAs functional parts at the micron level and optimized several printing parameters. This method yielded prints characterized by smooth surfaces and strong interlayer adhesion. However, EHD inkjet printing is associated with elevated costs [74]. In summary, while nozzle-based direct printing of LMPAs has demonstrated feasibility, several limitations persist. FDM, for instance, yields printed parts with reduced accuracy and suboptimal surface finish, while complex structures remain challenging to produce. On the other hand, EHD inkjet printing, while achieving superior surface quality, incurs higher costs.

2 Literature gap and scope of the present work

The novelty of our research lies in addressing the limitations identified in previous studies on LMPA 3D printing. While significant advancements have been made in nozzle-based direct printing of LMPAs, challenges such as poor surface finish, limited ability to print complex structures, and high costs associated with advanced printing techniques remain. Furthermore, the relationship between LMPAs' melting points and their mechanical, electrical, and energy absorption properties has not been thoroughly explored.

To address these challenges, Jiang et al. [75, 76] proposed a groundbreaking technique termed "low-melting-point alloys integrated extrusion additive manufacturing." This method introduces a novel FDM approach for the production of intricate LMPAs components, all at a reasonable cost. The fundamental idea is to utilize dual nozzles during FDM, one for extruding polymers and the other for injecting LMPAs. This innovative approach resulted in the successful fabrication of complex LMPAs components, integrated circuits, and 3D products. Additionally, it produced LMPAs/polymer composite components characterized by superior mechanical properties. Importantly, this research showcased how FDM, a cost-effective 3D printing technology, could be harnessed to create complex lattice structures, dental components, and bone structures using LMPAs.

Nevertheless, the properties of LMPAs with varying melting points, manufactured through integrated extrusion additive manufacturing, warrant further exploration. Such investigations hold the promise of unlocking broader applications in the realms of metal part design, energy harvesting and absorption, electrical circuits, and equipment.

In this paper, we embark on a comprehensive examination of LMPAs fabricated via integrated extrusion additive manufacturing, focusing on material testing. Our research will encompass LMPAs with differing melting points, scrutinizing several crucial properties: mechanical performance, electrical conductivity, and energy absorption properties. Additionally, our study will delve into diverse materials for inverse molds, aiming to ascertain the most accurate, convenient, economical, and environmentally friendly approach to fabricate LMPAs parts through integrated extrusion additive manufacturing.

Additionally, our study will delve into diverse materials for inverse molds, aiming to ascertain the most accurate, convenient, economical, and environmentally friendly approach to fabricate LMPAs parts through integrated extrusion additive manufacturing.

3 Materials and methods

3.1 Raw materials

In our comprehensive study, we aimed to delve into the intricate interplay between the melting points of LMPAs and their resulting effects on mechanical behaviors, energy absorption characteristics, and electrical conductivities. To achieve this, we meticulously selected raw LMPAs with a diverse range of melting temperatures for our experimental investigations. These carefully chosen LMPAs, each characterized by a distinct melting point, also played a pivotal role in assessing the maximum operating temperature that the reversed materials, namely polylactic acid (PLA) and polyvinyl alcohol (PVA), can endure during the LMPA manufacturing process through EAM.

LMPAs were purchased from Ding Tai Metal Material Factory, the same supplier as in our previous studies [75, 76]. And their properties are presented in Table 1.

To evaluate the impact of the printing materials used for the reversed parts on the precision of printed LMPAs components, we employed a systematic approach. For the reversed parts, we utilized two distinct printing materials, namely PLA and PVA, both sourced from Polymaker, China, renowned for their quality and consistency. The diameters of the PLA and PVA filaments used in our experiments were both 1.75 mm.

For the dissolution of PLA, we employed dichloromethane, sourced from RCI Labscan Limited in Thailand, with batch number 22020141. This solvent was chosen for its compatibility with PLA and its effectiveness in dissolving the reversed parts, ensuring accurate and finely detailed LMPAs.

3.2 Printing conditions

Specific printing parameters for PLA and PVA were meticulously configured to ensure optimal results. These

Table 1 Composition and ratio of metal elements in LMPAs with different melting points. (Source: Ding Tai Metal Material Factory, Dongguan, China)

Melting point °C	Pb % (lead)	Sn % (Tin)	Bi % (Bismuth)	Cd % (Cadmium)	In % (Indium)
47	22.6	8.3	44.7	5.3	19.1
57	18	11.6	49.4	–	21
70	25	12.5	50	12.5	–
82	43	–	50	7.0	–
100	30	18	52	–	–
120	–	–	–	25	75

parameters included a layer height of 0.15 mm, an infill density of 100%, a print speed of 60 mm/s, and bed temperatures set equal to the temperature of the printed LMPAs minus 10°C. Notably, the nozzle temperatures for PLA and PVA were maintained at 205°C and 215°C, respectively, to ensure precise and controlled extrusion. Taking into consideration the Arrhenius equation, as shown below, we have established a practice of setting the printing temperature for low melting point alloys approximately 10 degrees higher than their respective melting points with an injection speed of 0.8 mm^3/s. This temperature adjustment ensures that the viscosity of the alloy is sufficiently reduced, allowing it to flow smoothly inside the reversed part.

$$\eta = \eta_0 \cdot e^{-\frac{E}{kT}} \tag{1}$$

where η is the viscosity at temperature T, η_0 is the reference viscosity at a reference temperature, E is the activation energy for the flow process, k is the Boltzmann constant.

By employing this meticulously planned experimental approach, we aimed to shed light on the intricate relationships between LMPAs, their melting points, and the choice of printing materials, thereby contributing valuable insights to the field of materials science and engineering.

3.3 Design of test bars, lattice structures, TPMS structures, and their reversed parts

Tensile testing, a cornerstone in the realm of materials science and engineering, represents a fundamental procedure to evaluate a material's mechanical properties by subjecting it to controlled tension until it reaches failure. Within the domain of materials testing, the uniaxial tensile test stands as one of the most widely employed methods for assessing the behavior of isotropic materials. In alignment with recognized industry standards, this paper employs a meticulously designed test bar featuring a distinctive dog-bone shape, as specified by the guidelines established in [77]. This ensures that the tensile tests are executed with precision and adherence to established testing protocols.

In the pursuit of advancing energy absorption applications, particularly in comparison to other solid materials [78], metals hold a distinct advantage. Their innate properties make them well-suited for such endeavors, as noted by Lefebvre in [79]. Consequently, this paper delves into the realm of energy absorption through a series of compression tests conducted on lattice structures and TPMS structures crafted from LMPAs characterized by varying melting points.

In the case of lattice structures, our investigation centers around the octet lattice design, a structure meticulously crafted to explore the immense potential of LMPAs in the realm of energy absorption and harvesting, as eloquently outlined by Berger in [80]. The octet lattice structure adheres to the principles of a face-centered cubic (FCC) topology, as exemplified by a single unit cell prominently depicted in Fig. 1. The formation of the octet structure entails the artful stacking of octahedral cells, with each strut ingeniously shared by two neighboring cells. This geometric arrangement maximizes structural integrity and ensures efficient energy absorption, positioning LMPAs as promising candidates for applications demanding robust energy absorption properties.

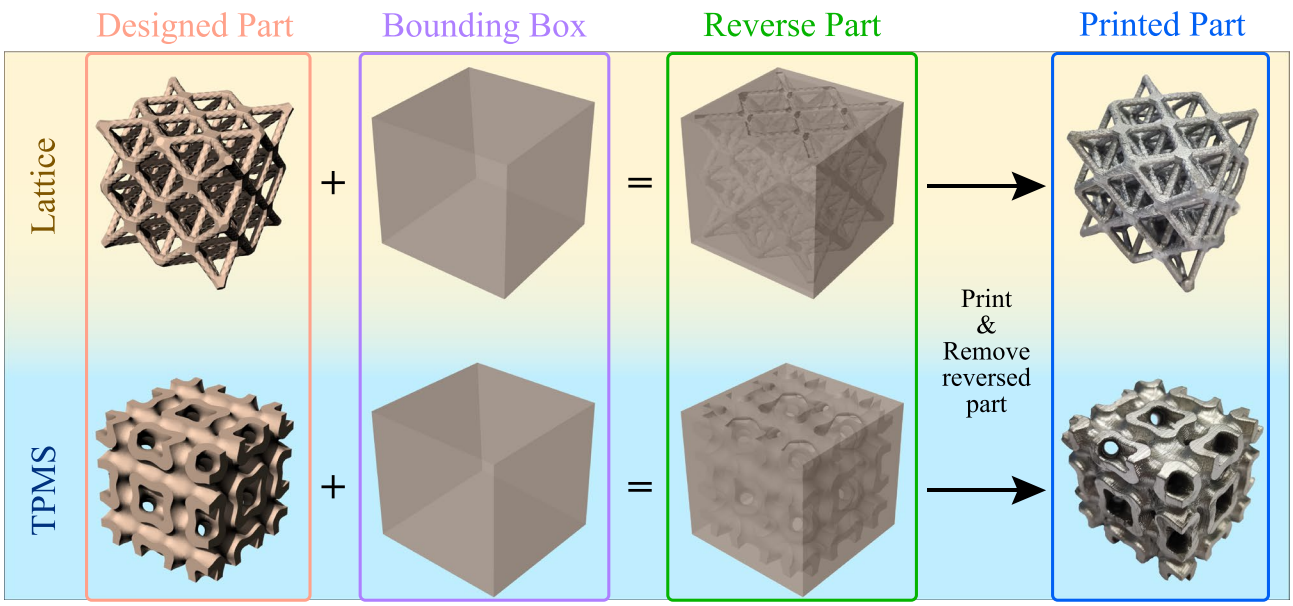

Fig. 1 Designed, reversed, and printed parts for lattice structures and TPMS structures

On the other hand, our exploration into TPMS structures unveils the intriguing potential of LMPAs in the realms of thermal energy storage and energy management, as meticulously elucidated by Ahmed in [81]. The TPMS structure under scrutiny exhibits a genus-four topology, presenting as a triply periodic minimal surface with remarkable characteristics, as aptly depicted in Fig. 1. Akin to a sphere adorned with handles that extend toward the vertices of a cube, this TPMS structure showcases exceptional properties conducive to thermal energy storage and efficient energy management. The unique design of the TPMS structure, coupled with the advantageous attributes of LMPAs, holds promise for innovative applications where precision energy control and management are paramount.

3.4 Test set-up and methods

The tensile tests and compression tests of lattice structure and TPMS structure are conducted using a CMT5105 universal Electromechanical Testing Machine from MTS Systems Corporation in Canada with a 2 kN load cell. For these tests, conventional and standardized test samples are created in Sect. 3.3. The tensile test and compression test were conducted at a controlled room temperature of 28 ± 2 °C and relative humidity of $85 \pm 5\%$.

For the tensile test, the specimens were clamped securely in the machine's grips, ensuring no slippage during testing. A pre-load of 0.1 N was applied to remove any slack and ensure proper alignment of the specimen along the loading axis. The tests were performed at a constant crosshead speed of 1 mm/min to capture the stress–strain behavior accurately. The tensile test continued until specimen failure, and data were recorded at a sampling rate of 10 Hz to capture the stress–strain curve in detail.

For compression tests, the specimens were positioned between two polished, hardened steel plates to ensure even distribution of the compressive load. The alignment of the specimen was checked carefully to avoid eccentric loading. A pre-load of 0.2 N was applied to ensure full contact between the specimen and the compression plates. The compression tests were performed at the same testing speed of 1 mm/min as the tensile tests. Load and displacement data were collected continuously, and the test was stopped either upon reaching the maximum displacement limit or specimen densification (where a large increase of load was observed with minor increased displacement).

To ensure the repeatability and accuracy of the results, calibration of the testing machine was conducted before each test series using standardized calibration blocks. Each test was repeated three times, and the data were averaged to minimize the effect of any anomalies. Statistical analysis, including standard deviation and confidence interval calculations, was performed on the measured properties to ensure the reliability of the results.

3.5 Manufacturing process

In the course of this study, an innovative approach to Extrusion Additive Manufacturing (EAM) integrated with Low-Melting-Point Alloys has been employed, offering new avenues for the fabrication of intricate LMPA components while maintaining cost-effectiveness. This method leverages the synergistic use of two distinct nozzles in the manufacturing process, representing a significant advancement in additive manufacturing techniques for LMPAs.

The fundamental principle underlying LMPAs EAM involves the application of dual nozzles during the fabrication process. One nozzle is dedicated to precisely extruding polymers such as PLA, PVA, and similar materials, while the second nozzle plays a pivotal role by injecting molten LMPAs into the component under production. Figure 2 illustrates the sequential operation of this pioneering manufacturing process.

During the polymer printing phase of component fabrication (Fig. 2a), Nozzle 1 is actively engaged. This phase progresses from left to right in the diagram as it systematically constructs the polymer segment of the component. Once the polymer section is completed, Nozzle 2 assumes the primary role, injecting molten LMPAs into the structure. As these LMPAs are introduced, they undergo rapid solidification, transforming into their final solid state as they cool below the characteristic melting point of the LMPAs used.

To bring these intricate LMPA parts to completion, meticulous post-processing steps are undertaken. This involves the removal of the polymer component by immersing the fabricated structure in an appropriate solvent. The choice of solvent depends on the polymer used; for instance, Dichloromethane effectively dissolves PLA components, while water serves as an effective solvent for PVA. Once the polymer component is removed, the printed LMPA components undergo further refinement, including cleaning and polishing, culminating in the production of finalized, high-quality LMPA products.

This novel EAM approach not only demonstrates its efficacy in cost-effective manufacturing but also showcases its versatility and precision in creating LMPA components with intricate geometries and unique properties. By presenting this methodology, our research contributes to advancing the field of materials engineering, opening up promising avenues for a wide range of applications in areas such as smart structures, electromagnetic shielding, biomedicine, thermal management, energy harvesting, and advanced electronics.

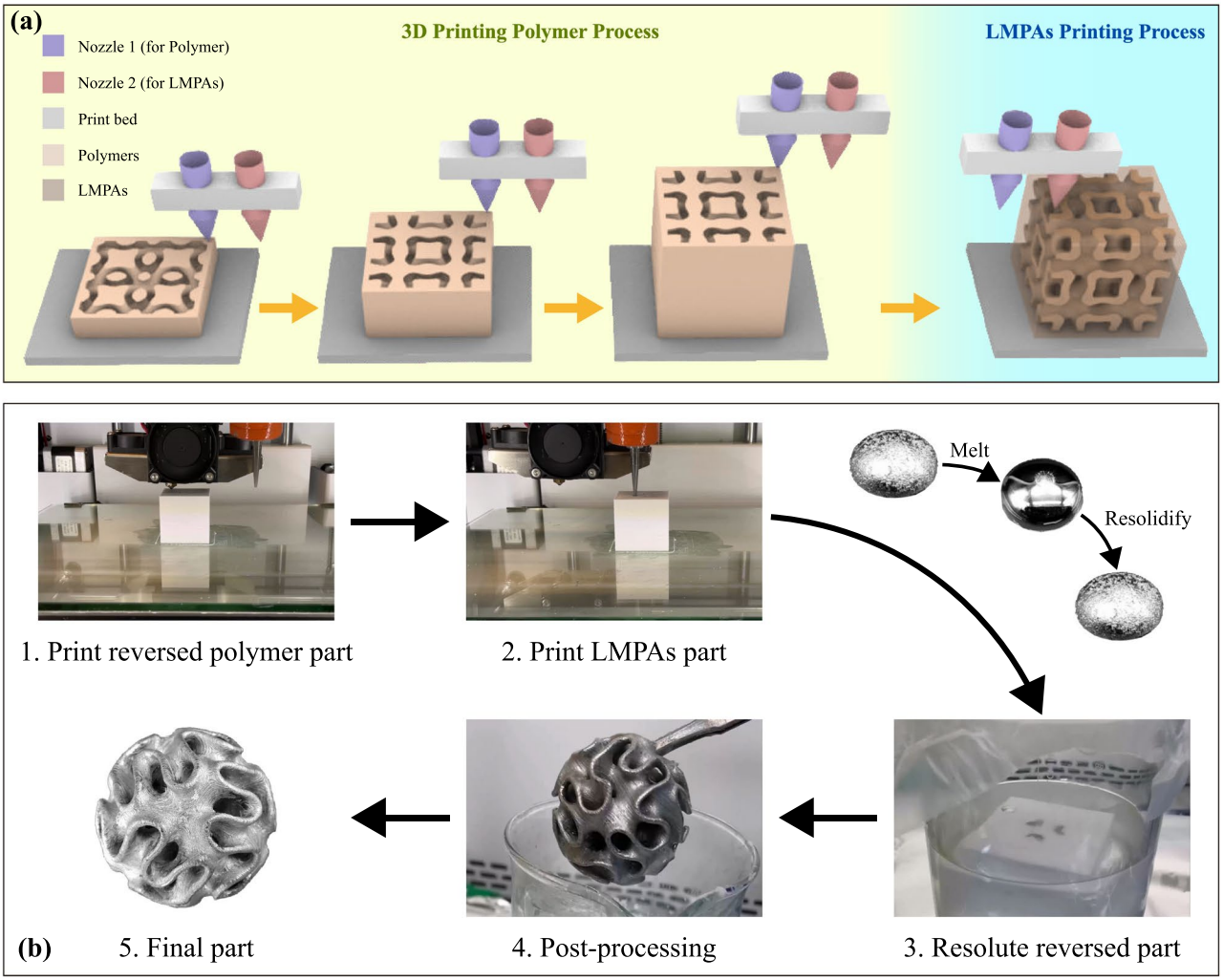

Fig. 2 Schematic diagram for manufacturing process of LMPAs integrated EAM. **a** Demonstration of printing process. **b** The whole workflow to produce the LMPA parts

4 Results and discussion

In this section, we present the test results and engage in a comprehensive discussion of the outcomes from our experimental investigations, encompassing tensile tests, compression tests of lattice structures and TPMS structures, as well as electrical conductivity tests. Additionally, our findings revealed that when the temperature exceeded 100 degrees (inclusive) during the 3D printing process of polymers, it led to polymer softening, rendering us unable to produce products with a melting point of low melting point alloy parts at or above 100 degrees. Therefore, there is no result for the tensile tests and compression tests of lattice structures and TPMS structures for the LMPAs whose melting points are above 100 degrees.

4.1 Test results for mechanical behavior

In the context of the tensile tests, our objective was to comprehensively assess the mechanical properties of LMPAs characterized by varying melting points, as visually depicted in Fig. 3a. The outcomes of these tests have unveiled intriguing insights into the behavior of these alloys under tensile stress, offering valuable information for engineering and material science applications.

Beginning with the LMPA featuring a melting point of 47°C, a noteworthy observation emerges. This particular alloy showcases relatively poor tensile performance when subjected to testing conditions. The primary contributing factor to this subpar performance is the alloy's exceptionally low melting point at or near room temperature. Consequently, the material exhibits characteristics akin to softness, resulting in a lower tensile strength. Such

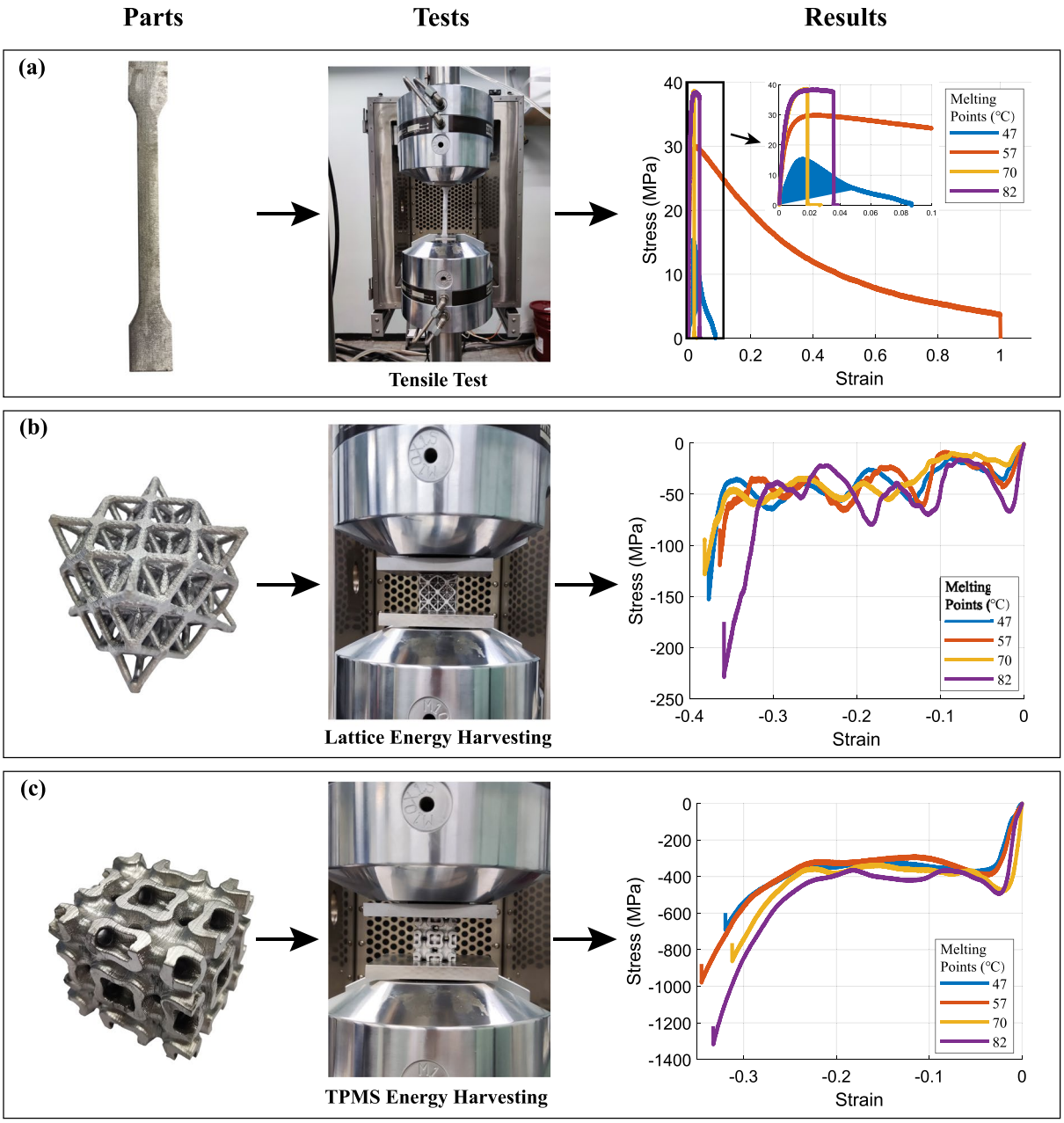

Fig. 3 Summary of test results for LMPAs with different melting points. **a** The results for the tensile test. **b** The results for the energy harvesting tests of lattice structures made of LMPAs. **c** The results for the energy harvesting tests of TPMS structures made of LMPAs

characteristics may limit its utility in applications that demand higher structural integrity and robustness.

Conversely, our investigations into the LMPA with a melting point of 57°C reveal a captivating aspect of its behavior. This alloy demonstrates exceptional ductility, surpassing the expectations of conventional materials. During tensile testing, this LMPA exhibits remarkable strains that extend well beyond 100%. This extraordinary ductility can be primarily attributed to the specific nature of the covalent bonds present in the alloy's composition. The combination of elements such as Indium (In), Tin (Sn), and Bismuth (Bi) leads to the formation of weaker covalent bonds, which contribute to the alloy's enhanced ductility and ability to undergo large deformations before fracturing. The presence of elements such as Indium (21%) and Tin (11.6%) in the alloy forms covalent bonds that are relatively weaker compared to the metallic bonds found in other alloys. These weaker covalent bonds allow for greater flexibility and elongation under tensile stress. Indium is known for its ductility and ability to form malleable covalent bonds. The 21% Indium content

Table 2 Mechanical properties of LMPAs with different melting points

Melting Points / °C	Young's Modulus (GPa)	Ultimate Strength (MPa)	Fracture Strain (%)
47	1.60	15.36	8.69
57	4.50	29.82	99.86
70	5.83	38.61	1.87
82	6.19	38.08	3.59

in the alloy enhances its ability to elongate significantly. Tin, with an 11.6% presence in the alloy, also contributes to the ductility of the LMPA by forming flexible covalent bonds. The addition of Bismuth (49.4%) helps to balance the structure, preventing brittleness and enhancing the overall ductility. This unique property opens doors to various applications that require materials capable of enduring significant deformation without fracture or failure.

As we shift our attention to LMPAs characterized by melting points of 70°C and 82°C, a different set of attributes comes into focus. These alloys, compared to their lower melting point counterparts, exhibit increased stiffness and resilience as shown in Table 2. They can withstand greater loads and possess enhanced resistance to deformation and structural changes. However, this heightened stiffness comes at a cost, as these alloys display reduced ductility. Consequently, they may be less suited for applications that prioritize flexibility and pliability over sheer stiffness.

In summary, our tensile test results have illuminated the diverse mechanical characteristics of LMPAs across different melting points. These findings provide a crucial foundation for tailoring the selection of LMPAs to suit specific engineering requirements. The choice between low melting point alloys for flexibility and higher melting point alloys for stiffness can significantly impact the performance and suitability of these materials in various applications.

4.2 Test results for energy absorption

The investigation into the energy absorption characteristics of lattice and TPMS structures yielded intriguing insights into the behavior of these structures across various manufacturing temperatures. Figure 3b, c provide a visual representation of the energy absorption results.

Upon a meticulous examination of Fig. 3b, c, a remarkable observation comes to light: the energy absorption effects of lattice and TPMS structures manufactured at different temperatures exhibit striking similarities. This uniformity in energy absorption behavior across a range of manufacturing temperatures underscores the robustness and reliability of LMPAs for energy absorption applications.

The lattice structures, designed with the octet lattice topology, and the TPMS structures, featuring the I-graph and wrapped package-graph (IWP) design, both showcase consistent energy absorption characteristics. This consistency suggests that the choice of manufacturing temperature, within the explored range, does not significantly alter the energy absorption capabilities of these structures.

The ability of LMPAs to maintain consistent energy absorption performance regardless of manufacturing temperature holds significant promise for applications where temperature fluctuations or manufacturing variability are common. This finding highlights the adaptability and versatility of LMPAs in contexts where energy absorption and dissipation are vital considerations.

In conclusion, the experimental results clearly indicate that the energy absorption effects of lattice and TPMS structures remain consistent across different manufacturing temperatures. This observation paves the way for the effective utilization of LMPAs in applications where energy absorption properties are paramount, providing engineers and researchers with a reliable and stable material option.

4.3 Test results for electrical conductivity

Table 3 provides a concise summary of the electrical resistivity measurements obtained for LMPAs with differing melting points. This data reveals intriguing trends that shed light on the electrical properties of these alloys and their relevance in various applications.

The tabulated data clearly demonstrates that electrical conductivity exhibits a notable dependency on the melting point of LMPAs. These findings can be attributed to the intricate interplay between the alloys' composition and their crystalline structure, which significantly influence their electrical behavior.

As we delve into the results, it becomes evident that LMPAs characterized by lower melting points, such as those at 47°C, 57°C, and 70°C, exhibit substantially higher electrical conductivity values. This heightened electrical conductivity in low melting point alloys can be attributed to several factors. Firstly, the elemental composition of these alloys,

Table 3 Electrical resistivity of LMPAs with different melting points

Melting Points / °C	Electrical Resistivity / $\Omega \cdot$ cm
47	0.0525×10^6
57	0.0487×10^6
70	0.0455×10^6
82	0.0328×10^6
100	0.0364×10^6
120	0.1229×10^6

which typically includes elements like lead (Pb), tin (Sn), bismuth (Bi), and indium (In), contributes to the formation of a conductive matrix. These elements possess inherent electrical conductivity properties, enhancing the overall conductive behavior of the alloy.

Additionally, the crystalline structure of LMPAs plays a pivotal role in their electrical performance. Lower melting point alloys tend to maintain a more amorphous or less ordered crystalline structure, which permits the flow of charge carriers (electrons) with greater ease. This increased disorderliness within the structure results in improved electrical conductivity.

In contrast, LMPAs with higher melting points, such as those at 82°C and 100°C, exhibit reduced electrical conductivity values. This reduction can be primarily attributed to the transformation of their crystalline structure into a more ordered, crystalline state as the temperature increases. In such ordered structures, the mobility of charge carriers is impeded, resulting in decreased electrical conductivity.

The standout observation from these electrical conductivity measurements is that the choice of LMPA with a specific melting point can be tailored to meet the requirements of various applications. For applications where high electrical conductivity is crucial, low melting point LMPAs are preferred. Conversely, applications where electrical conductivity is less critical may benefit from the mechanical properties offered by higher melting point LMPAs.

In conclusion, the electrical conductivity measurements presented in Table 3 highlight the pivotal role of melting point and alloy composition in shaping the electrical properties of LMPAs. These insights provide a foundation for informed material selection in diverse applications, where both electrical conductivity and mechanical characteristics are essential considerations.

4.4 Discussion

Our comprehensive experimental results have unveiled a wealth of knowledge regarding LMPAs with varying melting points, offering valuable insights for diverse applications. The relationship between melting point and mechanical behavior is evident, with lower melting points contributing to increased ductility but reduced stiffness, while higher melting points result in greater stiffness but diminished ductility. These findings underscore the importance of tailored LMPA selection based on specific application requirements. Remarkably, the energy absorption effects of lattice and TPMS structures manufactured at different temperatures exhibit striking similarities, highlighting the adaptability and versatility of LMPAs in contexts where energy absorption and dissipation are vital considerations. Furthermore, our electrical conductivity measurements reveal that LMPAs with lower melting points exhibit higher electrical conductivity, making them viable for applications requiring good electrical conduction properties. Overall, these findings underscore the importance of tailoring LMPAs based on the desired properties and applications, offering valuable insights for the development of novel materials and manufacturing techniques.

Compared with some other alloy (such as steel and iron-based alloys, nickel-based alloys, titanium-based alloys, and aluminum alloys) part made by selective laser melting (SLM) [82–87], the LMPA parts manufactured by extrusion-based additive manufacturing process offer several advantages, including ease of manufacturing and lower production costs. While the LMPA parts produced by this method have a lower Young's modulus compared to alloys printed by SLM, they exhibit higher fracture strain, making them suitable for applications requiring greater flexibility. Besides, LMPAs printed via extrusion-based additive manufacturing have mechanical properties that resemble those of photopolymers in terms of tensile strength. However, the extrusion-based process provides a practical and efficient alternative for producing LMPA parts, particularly for applications where the unique properties of LMPAs are advantageous.

By integrating LMPAs into an extrusion-based additive manufacturing process, we have developed a method that not only improves the precision and surface finish of printed parts but also allows for the fabrication of complex structures at a lower cost. The LMPA parts produced via extrusion-based additive manufacturing possess superior mechanical properties, specifically in terms of stiffness and fracture strain, compared to those reported in the reviewed literature [68–70, 73]. The enhanced stiffness observed in our LMPA parts can be attributed to one-piece molding enabled by extrusion additive manufacturing, which effectively increases the overall rigidity of the structure. Additionally, the larger fracture strain suggests that our method not only improves the load-bearing capacity but also enhances the ductility of the material, allowing for greater deformation before failure. In comparison to the literature [68–70, 73], where FDM and DED were mostly used, our extrusion-based approach offers a significant advantage in balancing stiffness and ductility. The parts fabricated in these studies generally exhibited lower fracture strain, indicating a higher likelihood of brittle failure. By contrast, our method provides a more robust solution, particularly for applications requiring both high stiffness and the ability to withstand larger deformations. Besides, compared with studies done by Hsieh et al. [68] and Parvanda & Kala [69] struggled with surface quality and the ability to produce complex shapes, our method achieves a high degree of precision and complexity. Additionally, compared to the

hybrid and resource-intensive processes reported by Deng et al. [64], our approach is simpler and more efficient, reducing the number of steps required while still delivering robust mechanical properties. Moreover, in contrast to the high costs associated with methods like EHD inkjet printing as discussed by Huang et al. [73], our approach offers a more economical solution without compromising on the quality or functionality of the LMPA parts. This makes our method particularly attractive for industrial applications where both cost and performance are critical.

5 Conclusions and future works

Our comprehensive experimental study has elucidated the mechanical behavior, energy absorption capabilities, and electrical conductivity of LMPAs with varying melting points. These findings provide valuable insights into the versatility and adaptability of LMPAs for diverse applications. We established a clear relationship between the melting point of LMPAs and their mechanical properties. Specifically, lower melting points enhance ductility but reduce stiffness, whereas higher melting points lead to greater stiffness but diminished ductility. This observation underscores the necessity of selecting LMPAs tailored to the specific requirements of the intended application. Additionally, the energy absorption properties of lattice and TPMS structures fabricated at different temperatures exhibit remarkable similarities, highlighting the robustness and reliability of LMPAs in contexts where energy absorption and dissipation are crucial. Electrical conductivity measurements further revealed that LMPAs with melting points of 47°C and 120°C exhibit higher electrical conductivity, making them well-suited for applications demanding superior electrical conduction properties. Our findings emphasize the importance of considering melting points and alloy compositions when selecting LMPAs for specific applications. The choice of LMPA can significantly impact the performance and suitability of materials in various contexts, including electronics, energy harvesting, and flexible circuits.

Additionally, our results pave the way for future research in several directions. Investigating advanced manufacturing techniques and processes can further enhance the mechanical and electrical properties of LMPAs, including refining the extrusion additive manufacturing process or exploring hybrid manufacturing approaches. Exploring the possibilities of combining LMPAs with other materials, such as polymers, to create composite materials with unique properties could also be fruitful. Optimizing manufacturing parameters, such as temperature, extrusion speed, and printing configurations, will help maximize the performance of LMPAs in specific applications. Focusing on the development of practical applications for LMPAs, leveraging their unique properties in fields like electronics, energy harvesting, and flexible circuits, is another promising direction. Furthermore, investigating the environmental impact of using LMPAs, including their recyclability and sustainability, is crucial to ensure responsible material usage.

Overall, our research provides a foundational understanding of LMPAs' mechanical and electrical properties, informing the development of novel materials and manufacturing techniques with broad industrial applications.

Acknowledgements This work is supported by the National Natural Science Foundation of China (No. 12371383), the Youth Innovation Key Research Funds for the Central Universities, China (YD0010002010), the Open Project Program of the State Key Laboratory of CAD&CG (Grant No. A2303), Zhejiang University, and the Strategic Priority Research Program of the Chinese Academy of Sciences, China (XDB0640000). For the purpose of open access, the authors have applied a Creative Commons Attribution (CC BY) licence to any Author Accepted Manuscript version arising from this submission.

Data availability The data supporting the findings of this study are available within the article.

Conflict of interest The authors declare that they have no known competing financial interests or personal relationships that couldhave appeared to influence the work reported in this paper.

References

1. Zhai X, Jin L, Jiang J (2022) A survey of additive manufacturing reviews, Mater Sci Additive Manuf 1 (4)
2. Jin L, Zhai X, Wang K, Zhang K, Wu D, Nazir A, Jiang J, Liao W-H (2024) Big data, machine learning, and digital twin assisted additive manufacturing: a review, Mater Design 113086
3. Arif ZU, Khalid MY, Zolfagharian A, Bodaghi M (2022) 4D bioprinting of smart polymers for biomedical applications: recent progress, challenges, and future perspectives, Reactive and Functional Polymers 105374
4. Park S, Shou W, Makatura L, Matusik W, Fu KK (2022) 3D printing of polymer composites: materials, processes, and applications. Matter 5(1):43–76
5. Singh S, Ramakrishna S, Berto F (2020) 3D Printing of polymer composites: a short review. Mater Design Process Commun 2(2):e97

6. Jin L, Yu S, Cheng J, Ye H, Zhai X, Jiang J, Zhang K, Jian B, Bodaghi M, Ge Q, Liao W-H (2024) Machine learning-driven forward prediction and inverse design for 4D printed hierarchical architecture with arbitrary shapes. Appl Mater Today 40:102373
7. Ligon SC, Liska R, Stampfl J, Gurr M, Mülhaupt R (2017) Polymers for 3D printing and customized additive manufacturing. Chem Rev 117(15):10212–10290
8. Stansbury JW, Idacavage MJ (2016) 3D printing with polymers: challenges among expanding options and opportunities. Dental Mater 32(1):54–64
9. Li X, Wang X, Mei D, Xu C, Wang Y (2024) Acoustic-assisted DLP 3D printing process for carbon nanofiber reinforced honeycomb structures. J Manuf Process 121:374–381
10. Jin L, Zhai X, Jiang J, Zhang K, Liao W-H (2024) Optimizing stimuli-based 4D printed structures: a paradigm shift in programmable material response, in: Sensors and Smart Structures Technologies for Civil, Mechanical, and Aerospace Systems 2024, Vol. 12949, SPIE, 2024, pp. 321–332
11. Alzyod H, Ficzere P (2023) Material-dependent effect of common printing parameters on residual stress and warpage deformation in 3D printing: A comprehensive finite element analysis study. Polymers 15(13):2893
12. Wei Q, Li H, Liu G, He Y, Wang Y, Tan YE, Wang D, Peng X, Yang G, Tsubaki N (2020) Metal 3D printing technology for functional integration of catalytic system. Nat Commun 11(1):1–8
13. Buchanan C, Gardner L (2019) Metal 3D printing in construction: a review of methods, research, applications, opportunities and challenges. Eng Struct 180:332–348
14. Das S, Bourell DL, Babu S (2016) Metallic materials for 3D printing. Mrs Bull 41(10):729–741
15. Duda T, Raghavan LV (2016) 3D metal printing technology. IFAC-PapersOnLine 49(29):103–110
16. Chen Z, Sun X, Shang Y, Xiong K, Xu Z, Guo R, Cai S, Zheng C (2021) Dense ceramics with complex shape fabricated by 3D printing: A review. J Adv Ceramics 10(2):195–218
17. Sajadi SM, Vásárhelyi L, Mousavi R, Rahmati AH, Kónya Z, KukoveczÁ, Arif T, Filleter T, Vajtai R, Boul P et al. (2021) Damage-tolerant 3D-printed ceramics via conformal coating, Science Advances 7 (28) eabc5028
18. Chen Z, Li Z, Li J, Liu C, Lao C, Fu Y, Liu C, Li Y, Wang P, He Y (2019) 3D printing of ceramics: a review. J Euro Ceramic Soc 39(4):661–687
19. Hwa LC, Rajoo S, Noor AM, Ahmad N, Uday M (2017) Recent advances in 3D printing of porous ceramics: a review. Curr Opin Solid State Mater Sci 21(6):323–347
20. Eckel ZC, Zhou C, Martin JH, Jacobsen AJ, Carter WB, Schaedler TA (2016) Additive manufacturing of polymer-derived ceramics. Science 351(6268):58–62
21. Weng Y, Li M, Wong TN, Tan MJ (2021) Synchronized concrete and bonding agent deposition system for interlayer bond strength enhancement in 3D concrete printing. Auto Construction 123:103546
22. Lim JH, Weng Y, Pham Q-C (2020) 3D printing of curved concrete surfaces using Adaptable Membrane Formwork. Construction Build Mater 232:117075
23. Weng Y, Li M, Ruan S, Wong TN, Tan MJ, Yeong KLO, Qian S (2020) Comparative economic, environmental and productivity assessment of a concrete bathroom unit fabricated through 3D printing and a precast approach. J Clean Product 261:121245
24. Kamble PP, Chavan S, Hodgir R, Gote G, Karunakaran K (2021) Multi-jet ice 3D printing, Rapid Prototyping Journal
25. Zheng F, Wang Z, Huang J, Li Z (2020) Inkjet printing-based fabrication of microscale 3D ice structures. Microsyst Nanoeng 6(1):1–10
26. Pronk A, Moonen Y, Ao C, Luo P, Wu Y (2017) 3D printing of ice, in: Proceedings of IASS Annual Symposia, Vol. 2017, International Association for Shell and Spatial Structures (IASS), pp. 1–8
27. Das AK, Agar DA, Rudolfsson M, Larsson SH (2021) A review on wood powders in 3D printing: processes, properties and potential applications. J Mater Res Technol 15:241–255
28. Le Duigou A, Castro M, Bevan R, Martin N (2016) 3D printing of wood fibre biocomposites: from mechanical to actuation functionality. Mater Des 96:106–114
29. Henke K, Treml S (2013) Wood based bulk material in 3D printing processes for applications in construction. Euro J Wood Wood Products 71(1):139–141
30. Johnson BN (2022) A sweet solution to complex microprinting. Science 378(6622):826–827
31. Leung PYV (2017) Sugar 3D printing: additive manufacturing with molten sugar for investigating molten material fed printing, 3D Printing and Additive Manufacturing 4 (1) 13–18
32. Ahmed N (2019) Direct metal fabrication in rapid prototyping: a review. J Manuf Process 42:167–191
33. Nandy J, Sarangi H, Sahoo S (2019) A review on direct metal laser sintering: process features and microstructure modeling. Lasers Manuf Mater Process 6(3):280–316
34. Soyama H, Takeo F (2020) Effect of various peening methods on the fatigue properties of titanium alloy ti6al4v manufactured by direct metal laser sintering and electron beam melting. Materials 13(10):2216
35. Murr LE, Gaytan SM, Ramirez DA, Martinez E, Hernandez J, Amato KN, Shindo PW, Medina FR, Wicker RB (2012) Metal fabrication by additive manufacturing using laser and electron beam melting technologies. J Mater Sci Technol 28(1):1–14
36. Gaytan SM, Murr LE, Medina F, Martinez E, Lopez M, Wicker RB (2009) Advanced metal powder based manufacturing of complex components by electron beam melting. Mater Technol 24(3):180–190
37. Li S-H, Kumar P, Chandra S, Ramamurty U (2022) Directed energy deposition of metals: processing, microstructures, and mechanical properties, International Materials Reviews 1–43
38. Ahn D-G (2021) Directed energy deposition (ded) process: state of the art. Int J Precision Eng Manuf-Green Technol 8(2):703–742
39. Tang Z-J, Liu W-W, Wang Y-W, Saleheen KM, Liu Z-C, Peng S-T, Zhang Z, Zhang H-C (2020) A review on in situ monitoring technology for directed energy deposition of metals. Int J Adv Manuf Technol 108(11):3437–3463
40. Rosli NA, Alkahari MR, bin Abdollah MF, Maidin S, Ramli FR, Herawan SG (2021) Review on effect of heat input for wire arc additive manufacturing process, Journal of Materials Research and Technology 11 2127–2145
41. Xia C, Pan Z, Polden J, Li H, Xu Y, Chen S, Zhang Y (2020) A review on wire arc additive manufacturing: monitoring, control and a framework of automated system. J Manuf Syst 57:31–45
42. Wang L, Xue J, Wang Q (2019) Correlation between arc mode, microstructure, and mechanical properties during wire arc additive manufacturing of 316l stainless steel. Mater Sci Eng 751:183–190
43. Li M, Du W, Elwany A, Pei Z, Ma C (2020) Metal binder jetting additive manufacturing: a literature review, J Manuf Sci Eng 142 (9)
44. Bai Y, Williams CB (2015) An exploration of binder jetting of copper, Rapid Prototyping Journal
45. Chen Q, Liang X, Hayduke D, Liu J, Cheng L, Oskin J, Whitmore R, To AC (2019) An inherent strain based multiscale modeling framework for simulating part-scale residual deformation for direct metal laser sintering. Additive Manuf 28:406–418
46. Lee W, Kim H, Kang I, Park H, Jung J, Lee H, Park H, Park JS, Yuk JM, Ryu S et al (2022) Universal assembly of liquid metal particles in polymers enables elastic printed circuit board. Science 378(6620):637–641

47. Zou Z, Chen Y, Yuan S, Luo N, Li J, He Y (2022) 3D printing of liquid metals: recent advancements and challenges, Advanced Functional Materials 2213312
48. Khondoker MA, Ostashek A, Sameoto D (2019) Direct 3D printing of stretchable circuits via liquid metal co-extrusion within thermoplastic filaments. Adv Eng Mater 21(7):1900060
49. Wang L, Liu J (2014) Liquid metal inks for flexible electronics and 3D printing: A review, in: ASME International Mechanical Engineering Congress and Exposition, Vol. 46445, American Society of Mechanical Engineers, p. V02BT02A044
50. Yu B, Liu L, Liu B, Zhao X, Deng W (2022) Printing of low-melting-point alloy as top electrode for organic solar cells, Advanced Optical Materials 2201977
51. Wang X, Li L, Yang X, Wang H, Guo J, Wang Y, Chen X, Hu L (2021) Electrically induced wire-forming 3D printing technology of gallium-based low melting point metals. Adv Mater Technol 6(11):2100228
52. Tan J, Low H (2018) Embedded electrical tracks in 3D printed objects by fused filament fabrication of highly conductive composites. Additive Manuf 23:294–302
53. Andersen K, Dong Y, Kim WS (2017) Highly conductive three-dimensional printing with low-melting metal alloy filament. Adv Eng Mater 19(11):1700301
54. Yu Y, Lu J, Liu J (2017) 3D printing for functional electronics by injection and package of liquid metals into channels of mechanical structures. MaterDesign 122:80–89
55. Swensen JP, Odhner LU, Araki B, Dollar AM (2015) Injected 3D electrical traces in additive manufactured parts with low melting temperature metals, in: 2015 IEEE International Conference on Robotics and Automation (ICRA), IEEE, pp. 988–995
56. Gozen BA, Tabatabai A, Ozdoganlar OB, Majidi C (2014) High-density soft-matter electronics with micron-scale line width. Adv Mater 26(30):5211–5216
57. Wang L, Liu J (2014) Compatible hybrid 3D printing of metal and nonmetal inks for direct manufacture of end functional devices. Sci China Technol Sci 57(11):2089–2095
58. Deng Y, Jiang Y, Liu J (2021) Low-melting-point liquid metal convective heat transfer: a review. Appl Thermal Eng 193:117021
59. Huang P, Wei G, Cui L, Xu C, Du X (2021) Numerical investigation of a dual-pcm heat sink using low melting point alloy and paraffin. Appl Thermal Eng 189:116702
60. Wang L, Liu J (2014) Liquid phase 3D printing for quickly manufacturing conductive metal objects with low melting point alloy ink. Sci China Technol Sci 57(9):1721–1728
61. Peng H, Guo W, Feng S, Shen Y (2022) A novel thermoelectric energy harvester using gallium as phase change material for spacecraft power application. Appl Energy 322:119548
62. Wang Q, Yu Y, Liu J (2018) Preparations, characteristics and applications of the functional liquid metal materials. Adv Eng Mater 20(5):1700781
63. Tang J, Wang J, Liu J, Zhou Y (2016) A volatile fluid assisted thermo-pneumatic liquid metal energy harvester. Appl Phys Lett 108(2):023903
64. Deng F, Nguyen Q-K, Zhang P (2020) Multifunctional liquid metal lattice materials through hybrid design and manufacturing. Additive Manuf 33:101117
65. Long F, Shao Y, Zhao Z, Fang M, Zhang Z, Guo J, Sun A, Ren Y, Cheng Y, Xu G (2022) Printable multi-stage variable stiffness material enabled by low melting point particles additives, Journal of Materials Chemistry C
66. Guo S, Lin R, Wang L, Lau S, Wang Q, Liu R (2019) Low melting point metal-based flexible 3D biomedical microelectrode array by phase transition method. Mater Sci Eng 99:735–739
67. Li B, Liu J, Gu H, Jiang J, Zhang J, Yang J (2019) Structural design of FDM 3D printer for low-melting alloy, in: IOP Conference Series: Materials Science and Engineering, Vol. 592, IOP Publishing, p. 012141
68. Hsieh PC, Tsai C, Liu BH, Wei W, Wang A-B, Luo RC (2016) 3D printing of low melting temperature alloys by fused deposition modeling, in: 2016 IEEE International Conference on Industrial Technology (ICIT), IEEE, pp. 1138–1142
69. Parvanda R, Kala P (2022) Process window identification for 3D printing low melting point alloy (LMPA) using fused deposition modelling (FDM), Rapid Prototyping Journal (ahead-of-print)
70. Ladd C, So J-H, Muth J, Dickey MD (2013) 3D printing of free standing liquid metal microstructures. Adv Mater 25(36):5081–5085
71. Yu Y, Liu F, Liu J (2017) Direct 3D printing of low melting point alloy via adhesion mechanism, Rapid Prototyping Journal
72. Yu Y, Liu F, Zhang R, Liu J (2017) Suspension 3D printing of liquid metal into self-healing hydrogel. Adv Mater Technol 2(11):1700173
73. Huang Y, Cao Y, Qin H (2022) Electric field assisted direct writing and 3D printing of low-melting alloy, Advanced Engineering Materials 2200091
74. Qu X, Li J, Yin Z, Zou H (2019) New lithography technique based on electrohydrodynamic printing platform. Organic Electron 71:279–283
75. Jiang J, Zhai X, Zhang K, Jin L, Lu Q, Shen Z, Liao W -H (2023) Low-melting-point alloys integrated extrusion additive manufacturing, Additive Manufacturing 103633
76. Jiang J, Zhai X, Jin L, Zhang K, Chen J, Lu Q, Liao W-H (2023) Design for reversed additive manufacturing low-melting-point alloys, Journal of Engineering Design 1–14
77. Standard test methods for tension testing of metallic materials (ASTM E8), Standard, ASTM International, West Conshohocken, PA (Dec. 2009)
78. Zhang K, Gao Q, Jiang J, Chan M, Zhai X, Jin L, Zhang J, Li J, Liao W-H (2024) High energy dissipation and self-healing auxetic foam by integrating shear thickening gel. Composites Sci Technol 249:110475
79. Lefebvre L-P, Banhart J, Dunand DC (2008) Porous metals and metallic foams: current status and recent developments. Adv Eng Mater 10(9):775–787
80. Berger J, Wadley H, McMeeking R (2017) Mechanical metamaterials at the theoretical limit of isotropic elastic stiffness. Nature 543(7646):533–537
81. Ahmed N, Barsoum I, Abu Al-Rub RK (2022) Numerical investigation on the effect of residual stresses on the effective mechanical properties of 3D-printed TPMS lattices, Metals 12 (8)1344
82. Gao S, Hu Z, Duchamp M, Krishnan PSR, Tekumalla S, Song X, Seita M (2020) Recrystallization-based grain boundary engineering of 316L stainless steel produced via selective laser melting. Acta Materialia 200:366–377
83. Fu J, Hu Z, Song X, Zhai W, Long Y, Li H, Fu M (2020) Micro selective laser melting of niti shape memory alloy: defects, microstructures and thermal/mechanical properties. Opt Laser Technol 131:106374
84. Impaziente F,. Giorleo L, Mazzucato F (2023) Selective laser melting of h13 tool steel powder: effect of process parameter on complex part production, Progress in Additive Manufacturing 1–14
85. Benedetti M, Perini M, Vanazzi M, Giorgini A, Macoretta G, Menapace C (2023)Atomized scrap powder feedstock for sustainable Inconel 718 additive manufacturing via LPBF: a study of static and fatigue properties, Progress in Additive Manufacturing 1–14
86. Ali MH, Sabyrov N, Shehab E (2022) Powder bed fusion-laser melting (PBF-LM) process: Latest review of materials, process parameter optimization, application, and up-to-date innovative technologies. Progress Additive Manuf 7(6):1395–1422

87. Bean GE, Witkin DB, McLouth TD, Zaldivar RJ (2020) Process gas influence on microstructure and mechanical behavior of Inconel 718 fabricated via selective laser melting. Progress Additive Manuf 5(4):405–417